On the Formation of Elliptical Galaxies

A. BURKERT

Max-Planck-Institut für Astrophysik
Karl-Schwarzschild Straße 1, D-85740 Garching bei München, Germany

1 Introduction

Elliptical galaxies are subdivided into three major groups (Bender et al. 1992; Fig. 1): giant ellipticals (gEs), compact ellipticals (cEs) and dwarf ellipticals (dEs).

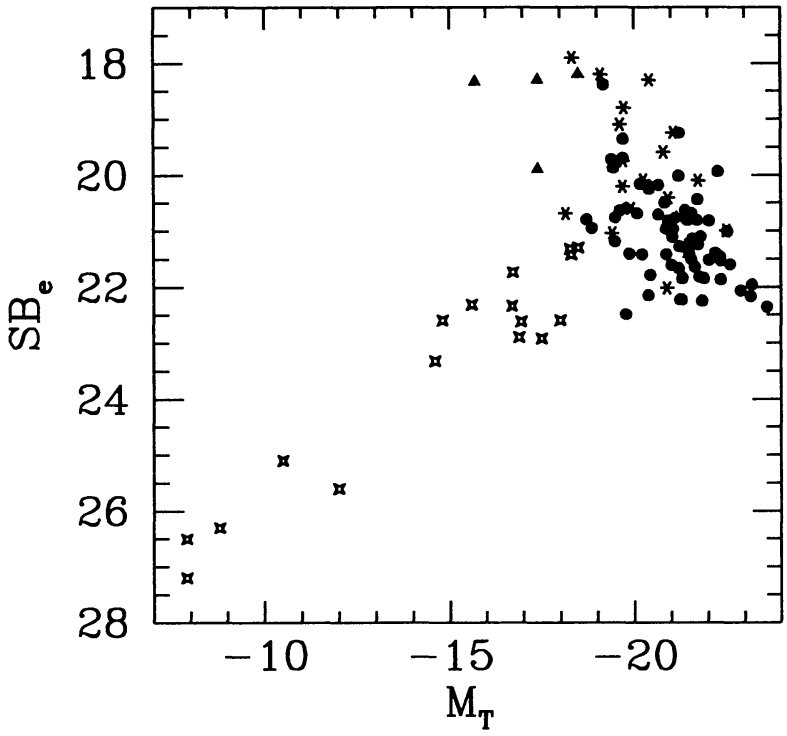

Figure 1: The effective surface brightness in the B band of dynamically hot stellar systems is shown as a function of their absolute visual magnitude in the B band. Source of values: Bender et al. 1992. Open stars are dwarf ellipticals, filled triangles are compact ellipticals, starred symbols are bulges and dots are giant ellipticals.

The gEs have absolute magnitudes $M_T \leq -18$ mag and masses $M \geq 10^{10} M_\odot$. Their surface densities are high and increase systematically with decreasing luminosity or mass. The dEs are characterised by surface densities which are orders of magnitudes smaller than for the gEs and which decrease systematically with decreasing mass. The cEs finally have masses similar to the more massive dEs, however

surface densities similar and even exceeding those of the giant ellipticals. It is important to note that high-density spheroids (gEs, cEs and bulges) are metal-rich systems whereas the low-density dwarfs have low metallicities, indicating differences in the star formation histories of both types of systems.

2 Supernova driven galactic winds

Is this phase transition from gEs to dEs a cosmological problem or a result of galactic evolution? The standard explanation is the formation of a galactic wind (Larson 1974; Dekel & Silk 1986; Yoshii & Arimoto 1987; Arimoto & Yoshii 1988) which in systems with low binding energies removes a large fraction of metal-enriched gas, by this leading to an expansion of the stellar component and to a low-metallicity, diffuse galaxy. One of the most popular wind models has been proposed by Yoshii and Arimoto (1987; YA87). In their scenario, a dwarf galaxy experiences an initial gravitational collapse of the gaseous protogalaxy and begins to form stars. Supernovae heat up the interstellar medium until its thermal energy exceeds its binding energy, leading to an outflow of the hot gas. This galactic wind removes the metal-enriched gas on a timescale which is short compared to the evolutionary timescale of the system. The decrease of the total mass due to the wind changes the binding energy of the system and leads to an expansion of the stellar system. In the case of a rapid gas removal the initial effective radius $r_{e,i}$ and the final radius $r_{e,f}$ are coupled with the total mass fraction f_{GW} which is lost in the wind:

$$\left(\frac{r_{e,f}}{r_{e,i}}\right) = \left(\frac{1 - f_{GW}}{1 - 2f_{GW}}\right). \tag{1}$$

Assuming a chemical closed box evolution (Edmunds 1990; Burkert 1993a) until the onset of the galactic wind, the final metallicity Z of the stellar component is

$$Z = -y \ln f_{GW} \approx -0.02 \ln f_{GW} \tag{2}$$

where $y \approx 0.02$ is the metal yield which determines the total mass of metals produced per unit mass of newly formed stars. For solar abundance ratios we now can derive the final iron abundance:

$$[Fe/H] = \log(Z/Z_{\odot}) \approx \log(-\ln f_{GW}) \tag{3}$$

where $Z_{\odot} \approx 0.02$ is the solar metal abundance. As f_{GW} increases with decreasing total mass, dwarf galaxies become more metal-poor with decreasing mass, in agreement with the observations.

Despite its attractivity as a simple description of dE-formation, the YA87-model has problems in explaining dwarf galaxies with low masses as these systems would become unbound for $f_{GW} > 0.5$ (eq. 1). If galaxies can only survive for $f_{GW} < 0.5$, equation 3 predicts a lower metallicity limit of $[Fe/H] > -0.16$ which is much larger than the observed metallicities of dEs. A possible solution might be the existence of a dark matter halo which would dominate the potential and confines these systems. Then, however, the galactic wind will not lead to an expansion as the mass which is lost in the wind will be small, compared to the total mass ($f_{GW} << 1$). One would then have to explain the low surface densities by another mechanism. The galactic wind might also occur on timescales which are long, compared to the dynamical

timescale. In this case, the system will expand adiabatically, that is $r_{e,f} = r_{e,i}/f_{GW}$. Under these circumstances one however cannot neglect energy dissipation, cooling and star formation during the wind phase which leads to a much more complex chemical and dynamical evolution which cannot be described by the equations (1) and (3).

3 The chemodynamical origin of high- and low-density ellipticals

The formation and strength of a galactic wind is regulated by energetic heating and cooling processes which play an important role during the formation and evolution of galaxies (Silk, 1985). The importance of galactic winds also demonstrates the intimate coupling of galactic dynamics and nucleosynthesis. Dynamical processes, on the one hand, affect the chemical evolution. Galactic heating- and cooling processes which regulate the winds are on the other hand a function of the metallicity of both, gas and stars again. Therefore, galactic chemistry and dynamics has to be considered simultaneously in so called *chemodynamical models.*

The chemodynamical model, proposed by Burkert & Hensler (1989) and Theis et al. (1992) takes into account two separate thermal gas phases (McKee & Ostriker 1977): cold molecular clouds (CM) are embedded in a hot, diffuse intercloud medium (ICM). The ICM and the CM are assumed to be in pressure equilibrium and the clouds move within the ICM like collision dominated particles.

Stars form only in the CM with a rate which is proportional to a power n of the local molecular gas density. The newly formed stars orbit within the galactic potential until they end as SNII (for masses $m \geq 10 M_{\odot}$), SNI or planetary nebulae. In addition, the high-mass stars can heat the surrounding gas through their UV-field and through the energy which is released in SN-explosions. They also eject metal-enriched gas into the ICM. This gas first has to cool and condense into clouds before new, metal- enriched stars can form.

Using his scenario, the chemodynamical calculations show an interesting dependence of the protogalactic evolution on the mass and density of the primordial fluctuation from which a galaxy forms. Figure 2 shows the cooling diagram of galaxies (Dekel & Silk 1986). The dashed curves indicate the baryonic number density of primordial 1σ to 3σ density fluctuations in an inflationary CDM universe with a baryonic mass fraction of 10%. The solid curve labeled $\tau_{cool} < \tau_{ff}$ encloses a region where the cooling timescale is shorter than the dynamical timescale. Molecular clouds, stars and galaxies can only form within a Hubble time from fluctuations which are located within this cooling region. This constraint leads to an upper mass limit for galaxies which is of the order of $10^{12} M_{\odot}$ (Blumenthal et al. 1984). Giant galaxies today have densities which are orders of magnitudes larger than their primordial density fluctuations, indicating a dissipation and collapse phase. Dwarf galaxies, on the other hand, have densities which are similar to their initial density. Therefore, these systems might not have contracted significantly but evolved self-regulated with energy dissipation being balanced by the energy input through high-mass stars.

This conclusion is strengthened by the chemodynamical models (Burkert & Hensler 1989) which show that there exists a critical density $n_{crit}(v)$ (thick lines

in Fig. 2) below which primordial density fluctuations do not collapse. These systems remain diffuse due to the balance of energy input and energy dissipation. They burn with a low, continuous star formation rate. Due to the shallow potential well a galactic wind arises early in the evolution of these systems. The mass loss is strongly correlated with the star formation rate and removes a large fraction of the metal-enriched hot ICM. This gas component results primarily from supernovae which eject the metals produced in high-mass stars. Its metallicity therefore is high, leading to a selective metallicity loss and by this to low-metallicity dwarf galaxies (Vader 1986, 1987). Note that through this mechanism almost all metals can be removed without loosing a large fraction of the total gas mass. As the mass loss occurs on timescales which are long compared to the dynamical timescale, the condition of a rapid gas removal does not apply and the systems remain gravitationally bound.

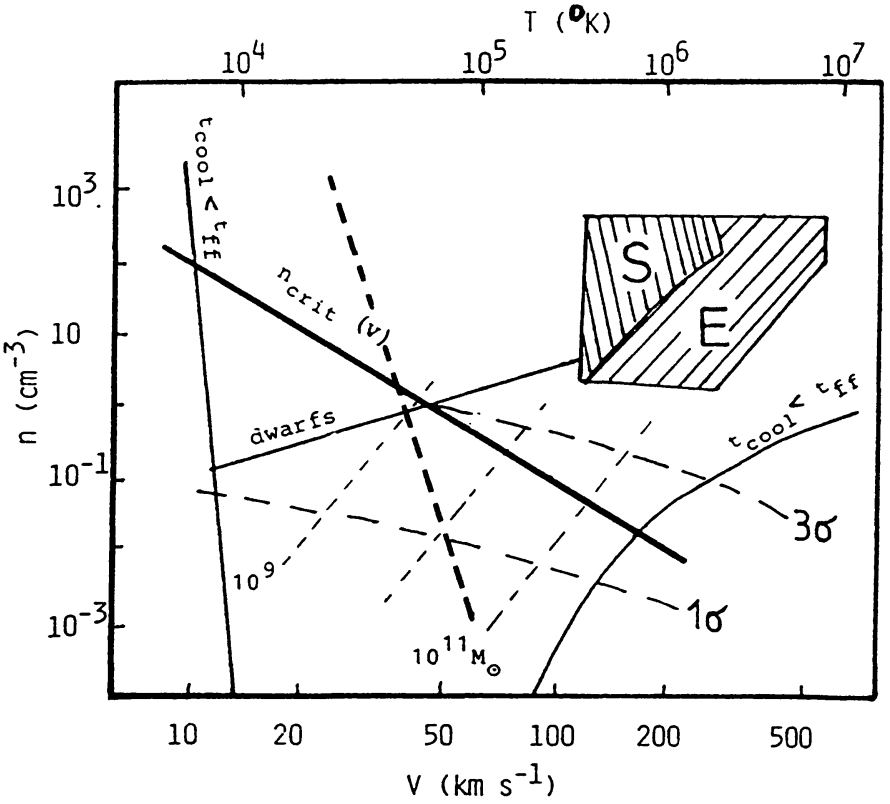

Figure 2: The gas number density versus the virial velocity or virial temperature is plotted for various morphological types of galaxies. The cooling curve $\tau_{cool} < \tau_{ff}$ confines the region inside which galaxies can form. The dotted lines represent systems of constant dark matter mass. The dashed curves show primordial 1σ to 3σ CDM density perturbations, assuming a baryonic mass fraction of 10%. The two thicker lines which cross the cooling region show the critical density for collapse assuming a star formation rate $d\rho_*/dt \sim \rho_g$ for the solid, thick line and $d\rho_*/dt \sim \rho_g^{1.5}$ for the dashed, thick line.

Systems with $n > n_{crit}$ dissipate their internal kinetic and thermal energy more efficiently, leading to a collapse phase. The gas density increases, triggering a vi-

olent star burst phase, which transforms most of the gas into stars and heats up the remaining gas, forming a giant elliptical with a high surface density which is embedded in a hot gaseous corona (Theis et al. 1992).

The critical collapse line n_{crit} crosses the region of primordial density fluctuations at a mass $M \approx 10^{10} M_{\odot}$ which is consistent with the upper mass limit for dwarf galaxies. Within the mass range $10^9 M_{\odot} \leq M \leq 10^{10} M_{\odot}$ primordial high-density fluctuations can still collapse and form compact stellar systems, whereas lower density fluctuations of the same initial mass evolve self-regulated and remain diffuse. The initial density might therefore represent the second parameter which in this limited range determines the evolution of protogalaxies. Compact ellipticals might then have formed from perturbations with initially exceptionally high densities whereas the dEs with similar masses formed in a low-density environment. This conclusion is consistent with the observational fact that almost all cEs are satellites of giant galaxies. This high-density environment was an ideal birth place for compact ellipticals. A more detailed discussion of cE-formation is given in Burkert (1994).

4 Dissipationless collapse models

According to the previous section, giant ellipticals formed from initial gaseous density fluctuations which experienced a violent collapse phase. A subsequent star burst transformed most of the gas into stars on a timescale which was shorter than the dissipation timescale, required for the gas to settle into the equatorial plane and form a rotationally supported disk galaxy.

Another frequently discussed scenario assumes that spiral galaxies formed first and spheroidal galaxies result from spiral-spiral mergers, as a secondary event (Toomre 1977). It was however shown by Hernquist (1992, 1993) that such a collisionless merger cannot explain the high phase space densities, observed in gEs if the spirals did not already contain elliptical-like massive, stellar bulges. Then, however, the formation of dense spheroidal stellar systems is not solved by the merger model as one would have to explain how the dense spheroids in the center of the spirals formed. In addition one would have to understand why it were only Sa-type spirals which merged and formed gEs. It is more likely, that the mergers occured at high redshifts where the spirals were still gaseous proto-disks. During the merger, the gas lost its angular momentum, cooled and settled into the inner regions of the merger remnant while condensing into a stellar system. In this case it is again a violent collapse with special, asymmetric initial conditions which leads to elliptical galaxies.

Within the framework of the collapse and merger picture the evolution of E-galaxies can be subdivided into two epochs: the initial, hydrodynamical collapse and star formation phase and the subsequent violent relaxation phase of the newly formed stellar system. Scientific work has focussed primarily on the late stellar dynamical phase, due to the lack of a consistent theory of star formation which would be required in order to understand the star formation phase. The basic idea was to find those initial conditions for the violently relaxing stellar systems which are required in order to explain the present structure of gEs. These initial conditions would then provide important insight into their early hydrodynamical and star formation phase.

The most important constraint for theoretical models of E-galaxy formation is

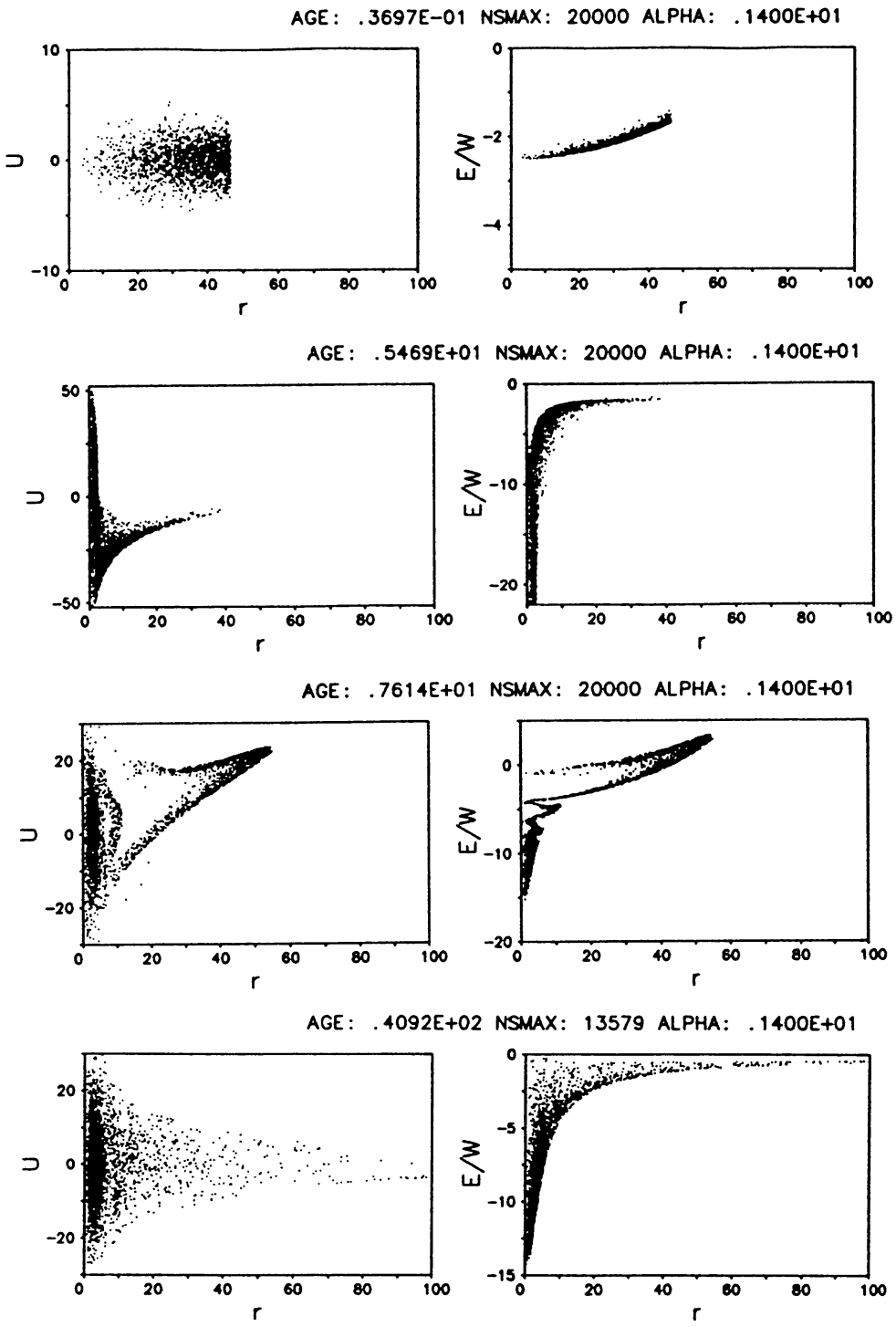

Figure 3: The evolution of a violently collapsing stellar system is shown. The left figures show the particle distribution in phase space with $u(r)$ the radial velocity at the radius r of the particle. The right figures show the normalized energy distribution of the particles. W is the absolute value of the mean potential energy per particle of the initial state.

their universal surface density profile which can be well described by the empirical relation (de Vaucouleurs 1948)

$$\log\left[\frac{\Sigma(R)}{\Sigma(R_e)}\right] = -3.331\left[\left(\frac{R}{R_e}\right)^{1/4} - 1\right]. \quad (4)$$

$\Sigma(R)$ is the surface density at a projected radius R assuming a constant M/L-ratio. R_e denotes the effective radius of the galaxy which determines the isophote that contains half the total luminosity. In a very influencial paper, van Albada (1982) showed that violently collapsing stellar systems relax towards an equilibrium state which fits the de Vaucouleurs law (eq. 4), independent of the detailed initial conditions. The most important requirement was an initially small virial coefficient $\eta_{vir} = 2E_{kin}/|E_{pot}| \leq 0.1$ where E_{kin} and E_{pot} are the total kinetic and potential energy, respectively. This result seems to confirm the importance of collisionless violent relaxation for the formation of E-galaxies.

As an example, figure 3 shows the violent relaxation of the standard model: an initially homogeneous, spherically symmetric stellar system with an initial virial coefficient $\eta_{vir} = 0.1$. Initially, the test particles are distributed randomly so as to produce a velocity distribution function

$$f(r,v) = \frac{\rho_0}{(2\pi\sigma^2)^{1.5}} \exp\left(-0.5\frac{v^2}{\sigma^2}\right). \quad (5)$$

ρ_0 is the initial density. The velocity dispersion σ determines the initial virial coefficient:

$$\eta_{vir} = \frac{5}{3}\frac{R\sigma^2}{GM} \quad (6)$$

where M is the total mass and R is the initial radius of the system. Due to the small initial virial coefficient the system experiences a strong collapse phase. The collective infall of stars leads to a central compression and to a deep inner potential well. Note that due to the infall the stellar energy changes strongly as a result of the time variation of the gravitational potential. After one collapse timescale most of the stars have crossed the center and the system re-expands again, by this lifting 33% of all the test particles to orbits with a positive total energy. These stars are lost. The bound stars turn around again at the outer edge of the potential well and fall back into the center. After a few free fall times τ_{ff} the system achieves a virial equilibrium state with $\eta_{vir} = 1$.

Figure 4 shows the stellar energy distribution, that is the number of stars with a normalized energy E/W at the beginning (t=0) and after 10 free-fall times. The final energy distribution differs strongly from the initial state as a result of violent relaxation which redistributes the energy of the particles due to the strong changes in the potential during the first free-fall time (Lynden-Bell 1967). As violent relaxation erases the information about the initial state we can hope that the virial equilibrium state is independent of the initial conditions and might explain the universal $r^{1/4}$-profiles of E-galaxies. Note, that in this case the brightness profiles of ellipticals do not contain much information about the initial state from which these systems formed.

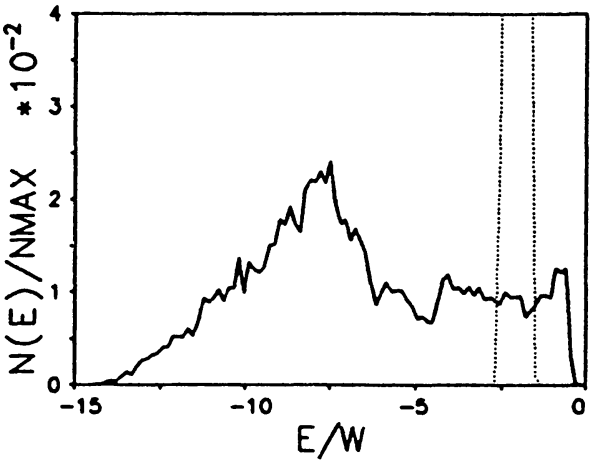

Figure 4: The normalized energy distribution of the stellar system is shown for the initial state (dotted line) and the virialized, final state (dashed line).

The surface density profile $\Sigma(R)$ of the standard model is plotted in figure 5a. Σ was determined by binning the projected particle distribution into centered ellipsoidal rings. In agreement with the models of van Albada (1982) and Burkert (1990) the outer region follows a de Vaucouleurs law whereas the inner part has a characteristic, polytrope-like structure which is not observed in E-galaxies. This result is actually expected from Liouvilles theorem which states that the microscopic phase space density $f(\vec{x}, \vec{v}, t)$ of a collisionless stellar system is a conserved quantity. Integrating over a finite phase space volume D one can derive a macroscopic phase space density

$$F = \int_D f d^3x d^3v \tag{7}$$

which cannot exceed the maximum microscopic phase space density f_{max}. As the de Vaucouleurs law leads to an inwards increasing macroscopic phase space density (Burkert 1990) the structure of a stellar system with an $r^{1/4}$-law in the outer region must change at the critical core radius r_{core} where

$$F(r_{core}) = f_{max} = \frac{\rho_0}{(2\pi\sigma^2)^{1.5}}. \tag{8}$$

Inside this degenerate core region the system cannot follow the universal de Vaucouleurs profile of the envelope. Here the structure depends strongly on the microscopic phase space density and by this on the initial conditions.

The effect of the central degeneracy can be strongly reduced if one starts from centrally condensed initial states which have regions of high microscopic phase space densities. This was demonstrated by Aguilar & Merritt (1990) who studied the cold collapse of stellar systems with initial density distributions $\rho \sim r^{-1}$. These initial conditions lead to a better agreement with the $r^{1/4}$-law than initially homogeneous conditions (Figure 5b).

Van Albada (1982) and May & van Albada (1984) argued that the angular momentum distribution of initially spherically symmetric systems is partly conserved, which has an affect on the universality of the final equilibrium state. Initially clumpy

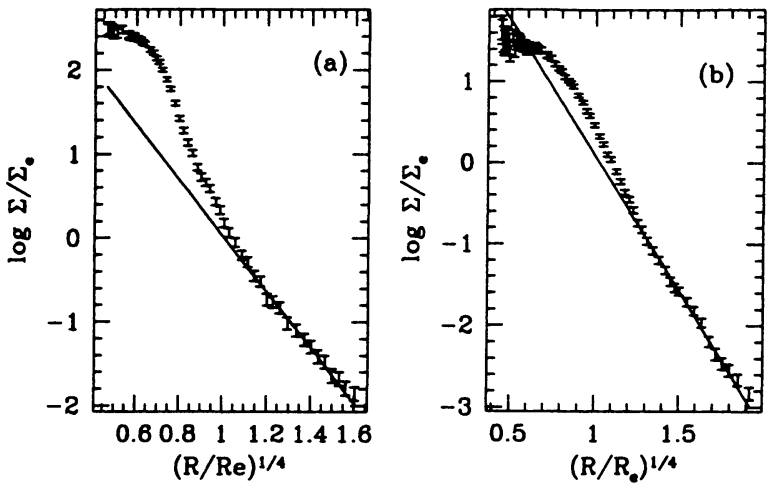

Figure 5: The equilibrium surface density distribution, normalized to the effective surface density Σ_e is shown for the initially spherically symmetric, collapse models with constant initial density (Fig. 5a) and an initial r^{-1} density profile (Fig. 5b). The error bars indicate the expected statistical 2σ errors. The solid line represents the best $r^{1/4}$-fit.

conditions could lead to efficient angular momentum redistribution and by this to more universal final states, in better agreement with an $r^{1/4}$-law. This would indicate that most ellipticals formed through the violent merging of small stellar subsystems, in agreement with cosmological cold dark matter simulations.

Figure 6 shows the final surface density profile of an initially clumpy, cold stellar system. Here we adopt the same initial conditions as in model C3 of van Albada (1982): 20 homogeneously filled spheres of radius 0.4 are placed inside a volume of radius 1. The stars of each clump move collectively with the assigned clump velocity which is chosen such that $\eta_{vir} = 0.1$. In this case no degenerate core is visible anymore and the de Vaucouleurs law fits the profile over a large radius range.

4.1 Do ellipticals have $r^{1/4}$-law profiles?

As the universal surface brightness distribution is used as an important constraint for theoretical models of E-galaxy formation one has to investigate how well ellipticals actually fit the $r^{1/4}$-law. In fact, the brightness profiles observed by Schombert (1986, 1987) show strong deviations from a perfect de Vaucouleurs law in the inner and outer regions. Therefore it is important to understand whether there exists a common radius range within which equation 4 fits all ellipticals and to specify the accuracy of this fit. This question has been investigated by Burkert (1993) who studied the photometric surface brightness profiles of a large sample of elliptical galaxies. He found that all ellipticals, independent of their global parameters, fit the de Vaucouleurs law within the same effective radius range $0.1R_e \leq R \leq 1.5R_e$ with an error

$$\Delta \log \Sigma = \log \Sigma - \log \Sigma_{1/4} \leq 0.08. \qquad (9)$$

$\Sigma_{1/4}$ is the perfect $r^{1/4}$-law and Σ denotes the observed surface density, assuming a

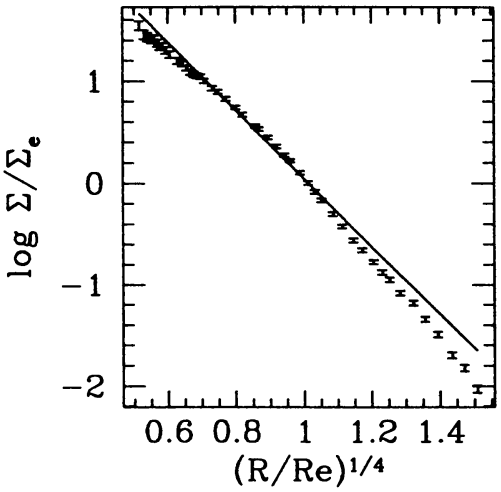

Figure 6: The surface density distribution of the clumpy collapse model is shown. The solid line indicates the best $r^{1/4}$-fit.

constant mass-to-light ratio. The scale length R_e is defined consistently through the slope of the best fitting $r^{1/4}$-law through the data points within the above specified radius range:

$$R_e = \left(\frac{-3.331}{d \log(\Sigma_{1/4})/dR^{1/4}} \right)^4 . \tag{10}$$

Note that the deviations from a perfect $r^{1/4}$-law lead to values for R_e which can deviate from the projected half-mass radius by a factor of 2. Burkert showed that E-galaxies do not have universal brightness profiles for $R > 1.5R_e$ and $R < 0.1R_e$.

Given these observations we now can analyse again the surface brightness profiles of cold collapse models. The solid lines in figure 5 show the best fitting $r^{1/4}$-law for the equilibrium surface density profiles of the spherically symmetric collapse models. The outer regins can be fitted nicely by a de Vaucouleurs law. This $r^{1/4}$-law however cannot fit the region inside R_e. If we try to fit the inner region of the centrally condensed model (Fig. 7) the slope $d \log \Sigma / dR^{1/4}$ becomes more negative, leading to a smaller effective radius. Therefore the fit lies again outside the corresponding scale radius R_e. In summary, it is not possible to find a good fit to the de Vaucouleurs profile within the radius range $0.6 \leq (R/R_e)^{1/4} \leq 1.1$. Additional test calculations show a similar result for other spherically symmetric density distributions. Very special initial density profiles are required in order to get a good $r^{1/4}$-fit in the observed radius range (see section 5). We therefore have to conclude that the violent relaxation of initially centrally condensed, spherical stellar system cannot explain the universal profiles of elliptical galaxies.

Could the de Vaucouleurs profile be a result of the angular momentum redistribution of initially clumpy stellar systems? The best fitting $r^{1/4}$-profile within the right radius range for van Albada's C3 model is shown in figure 6. In this case the surface density gradient decreases and by this the effective radius of the best fitting $r^{1/4}$-law increases with decreasing radius. It is therefore possible to find a fit within $0.6 \leq (R/R_e)^{1/4} \leq 1.1$. The maximum deviation from the perfect $r^{1/4}$-law

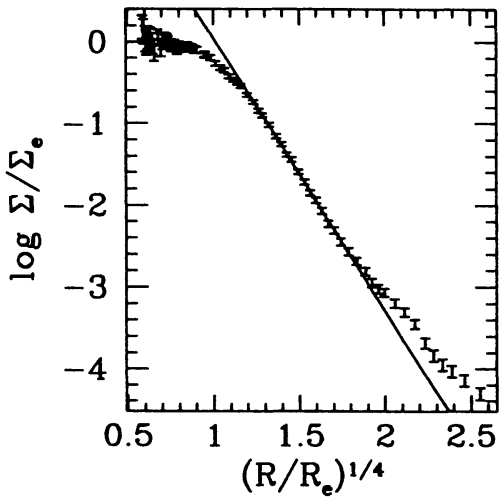

Figure 7: The best $r^{1/4}$-fit to the inner region of the initially centrally condensed, spherically symmetric model is shown.

is $\Delta \log \Sigma = 0.24$ and by this a factor of 3 larger than the observed maximum deviations in E-galaxies. Model C3 is one of the best clumpy initial conditions found by van Albada. Test calculations demonstrate that small variations of the initial distribution of clumps lead to large variations in $\Delta \log \Sigma$ with most cases having even larger deviations than the C3-model and only some special cases leading to a better agreement with the de Vaucouleurs law. We therefore have to conclude that neither violent relaxation nor angular momentum redistribution alone can correctly describe the formation of the universal surface brightness profiles of elliptical galaxies, independent of the initial conditions.

5 The central condensation model

The results of section 4 indicate that the stellar component of ellipticals might already have formed with the right universal density profile which is required to lead to a $r^{1/4}$-law in the observed radius range. We then have to investigate which mechanism could lead to such a universal initial state.

Within the framework of the central condensation model we assume that proto-ellipticals formed through the hierarchical merging of smaller subunits which consisted of gas, being embedded inside a dark matter halo or from the merging of gaseous protodisks with dark matter halos. During the merger, the gas of each subunit decoupled from the dark matter halo and accumulated in the center of the newly formed protogalaxy. The collisionless dark matter halos merged without dissipation and formed a new, virialized, extended dark matter component with a typical scale length which is approximately 10 times the scale length of the baryonic component (Carlberg 1986). In contrast to the standard collapse model we assume that the gas did not form stars efficiently while settling into the core of the newly formed dark matter halo. A similar scenario was proposed by Murray & Lin (1989) and Lin & Murray (1992) who argued that self-regulated high-mass star formation could efficiently heat the protogalactic gas during the settling period, keeping the gas at

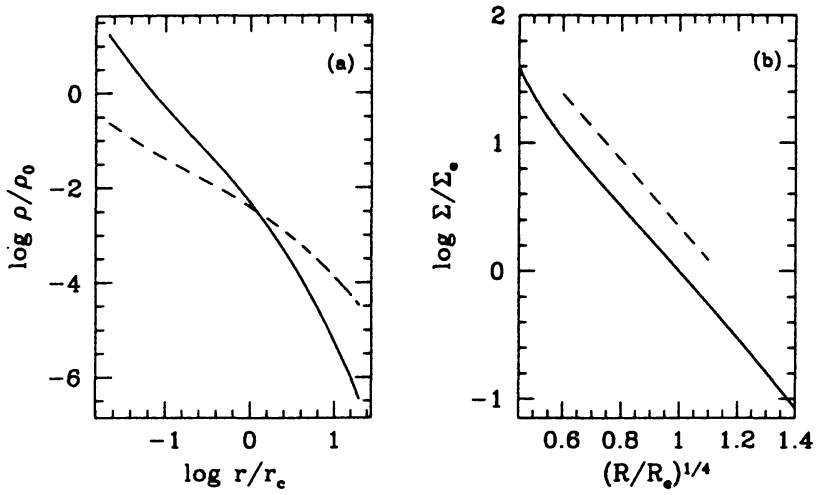

Figure 8: The density distribution (Fig. 8a) of the baryons (solid line) and the dark matter halo (dashed line), normalized to the central dark matter density ρ_0 is shown as a function of r, normalized to the dark matter core radius r_c. Figure 8b compares the surface density profile of the isothermal gas sphere with the $r^{1/4}$-law (dashed line).

an almost constant temperature $T \approx 10^4 K$. The gas finally achieved an isothermal equilibrium state with sound velocity c_g inside the core region of the dark matter component. In this region one can approximate the dark matter density distribution by an isothermal sphere with a velocity dispersion $\sigma_{DM} > c_g$. As the gas and the dark matter are confined by the same gravitational potential Φ, their density distributions are coupled through the hydrostatic equation:

$$\frac{c_g^2}{\rho_g}\frac{d\rho_g}{dr} = -\nabla\Phi = \frac{\sigma_{DM}^2}{\rho_{DM}}\frac{d\rho_{DM}}{dr} \tag{11}$$

The solution of equation 11 is

$$\rho_g = A(\rho_{DM})^{\sigma_{DM}^2/c_g^2} \tag{12}$$

where A is a constant.

Given the central gas density $\rho_g(r=0)$, Poisson's equation can be used in order to calculate the radial baryonic and dark matter density distribution:

$$\frac{1}{r^2}\frac{d}{dr}\left(r^2\frac{d\ln\rho_g}{dr}\right) = \frac{4\pi G}{c_g^2}(\rho_g + \rho_{DM})\,. \tag{13}$$

As an example, figure 8a shows the density distribution of the baryons and the dark matter for centrally condensed, gaseous spheres with a temperature ratio $\sigma_{DM}^2/c_g^2 \sim 2$. The gas has a density distribution which is equal to the profile of a self-gravitating isothermal sphere in the inner region and has a density cut-off at the core radius of the dark matter halo where the dark matter density begins to decrease as $\rho_{DM} \sim r^{-2}$. The surface density profile of the baryons follows nicely a de Vaucouleurs law inside R_e (Fig. 8b). Note, that in this model the dark matter core radius determines the scale length of the baryonic system.

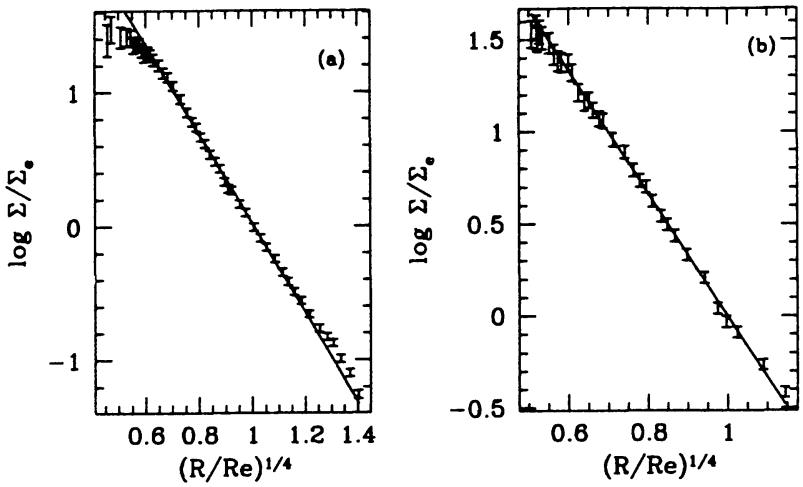

Figure 9: The equilibrium surface density distribution of an initially virialised stellar system ($\eta_{vir} = 1$; Fig. 9a) and an initially violently collapsing system ($\eta_{vir} = 0.1$; Fig. 9b) are shown. Both models started with a truncated, isothermal sphere like density distribution as shown in figure 8.

In the model of Lin and Murray (1992) the gas becomes thermally unstable after settling into the core region and forms a stellar system which initially has the same density distribution as the gas due to the fact that the cooling timescale is shorter than the dynamical timescale. If the gas looses its pressure support during the star formation phase, the stellar system is born with a small virial coefficient $\eta_{vir} \leq 1$. Figure 9 shows the final equilibrium state of two stellar systems with different initial virial coefficients, however with the same initial density distribution, as shown in figure 8. The surface profiles indeed fit the $r^{1/4}$-profile perfectly within the observed radius range.

6 Conclusions

The results of our chemodynamical models lead to a classification of elliptical galaxies into systems with an initial violent collapse and dissipation phase ($n > n_{crit}$, $M > 10^{10} M_{\odot}$) and systems which evolved self-regulated ($n < n_{crit}$, $M < 10^{9} M_{\odot}$). Giant ellipticals formed through a collapse, leading to high surface densities whereas the dwarf galaxies still remembered their initial densities and formed diffuse objects. Within a limited mass range ($10^{9} M_{\odot} \leq M \leq 10^{10} M_{\odot}$), high density systems (compact ellipticals) and low density systems (dwarf ellipticals) could form simultaneously, depending on the initial density fluctuation. The models predict that the birth places of cEs are exceptionally high density regions. This result might explain the observation that almost all cEs are satellites of massive galaxies.

We then have investigated the question whether the stellar component of gEs formed already prior, during or after the merging, dissipation and collapse phase of the protogalaxy. It has been shown that dissipationless violent relaxation and angular momentum redistribution cannot explain the universality of the surface brightness profiles of giant ellipticals. The collapse therefore occured prior to the

star formation event. The central condensation model assumes that the primordial gas settled into the core of the dark matter halos and formed an isothermal sphere which lateron condensed into stars. Stellar systems which formed in this way would indeed show the right universal brightness profiles which are observed in elliptical galaxies. Additional late infall of high-angular momentum gas might lead to the formation of a galactic disk around some of the less massive ellipticals which then would be classified as the bulges of spiral galaxies. Thus, ellipticals and bulges might trace directly the core radii and core masses of their dark matter halos providing important information on the nature of dark matter in galaxies.

ACKNOWLEDGEMENTS

I would like to thank R. Bender, G. Hensler, M. Steinmetz and C. Theis for enlightning discussions. Special thanks go to L. Hernquist for making available his TREECODE. All calculations have been performed on the Cray YMP 4/64 of the Rechenzentrum Garching.

REFERENCES

Arimoto, N., Yoshii, Y.: 1987, *Astr. Astrophys.* **173**, 23.
Aguilar, L.A., Merritt, D.: 1990, *Astrophys. J.* **354**, 33.
Bender, R., Burstein, D., Faber, S.M.: 1992, *Astrophys. J.* **399**, 462.
Blumenthal, G.R., Faber, S.M., Primack, J.R., Rees, M.J.: 1984, *Nature* **311**, 517.
Burkert, A., Hensler, G.: 1989, in "Evolutionary Phenomena in Galaxies", ed. J.E. Beckman, B.E.J. Pagel, Cambridge, p.230.
Burkert, A.: 1990, *Mon. Not. R. astr. Soc.* **247**, 152.
Burkert, A.: 1993a, *Journal Phys. G*, **19**, 171
Burkert, A.: 1993b, *Astr. Astrophys.* **278**, 23.
Burkert, A.: 1994, *Mon. Not. R. astr. Soc.* **266**, 877.
Carlberg, R.G.: 1986, *Astrophys. J.* **310**, 593.
Dekel, A., Silk, J.: 1986, *Astrophys. J.* **303**, 39.
de Vaucouleurs, G.: 1948, *Ann. Astrophys.* **11**, 247.
Edmunds, M.G.: 1990, *Mon. Not. R. astr. Soc.* **246**, 678.
Hernquist, L.: 1992, *Astrophys. J.* **400**, 460.
Hernquist, L.: 1993, *Astrophys. J.* **409**, 548.
Larson, R.B.: 1974, *Mon. Not. R. astr. Soc.* **169**, 229.
Lin, D.N., Murray, S.D.: 1992, *Astrophys. J.* **394**, 523.
Lynden-Bell, D.: 1967, *Mon. Not. R. astr. Soc.* **136**, 101.
May, A., van Albada, T.S.: 1984, *Mon. Not. R. astr. Soc.* **209**, 15.
McKee, C.F., Ostriker, J.P.: 1977, *Astrophys. J.* **218**, 148.
Murray, S.D., Lin, D.N.C.: 1989, *Astrophys. J.* **339**, 933.
Schombert, J.M.: 1986, *Astrophys. J.-Suppl. Ser.* **60**, 603.
Schombert, J.M.: 1987, *Astrophys. J.-Suppl. Ser.* **64**, 643.
Silk, J.: 1985, *Astrophys. J.* **297**, 9.
Theis, C., Burkert, A., Hensler, G.: 1992, *Astr. Astrophys.* **265**, 465.
Toomre, A.: 1977, in *The Evolution of Galaxies and Stellar Populations*, p.401, ed. Tinsley, B.M. & Larson, R., New Haven: Yale Univ. Obs..

Vader, P.: 1986, *Astrophys. J.* **305**, 669.
Vader, P.: 1987, *Astrophys. J.* **317**, 128.
van Albada, T.S.: 1982, *Mon. Not. R. astr. Soc.* **201**, 939.
Yoshii, Y., Arimoto, N.: 1987, *Astr. Astrophys.* **188**, 13.